Cell Reports
Physical Science

CellPress
OPEN ACCESS

Article

Competition between triplet pair formation and excimer-like recombination controls singlet fission yield

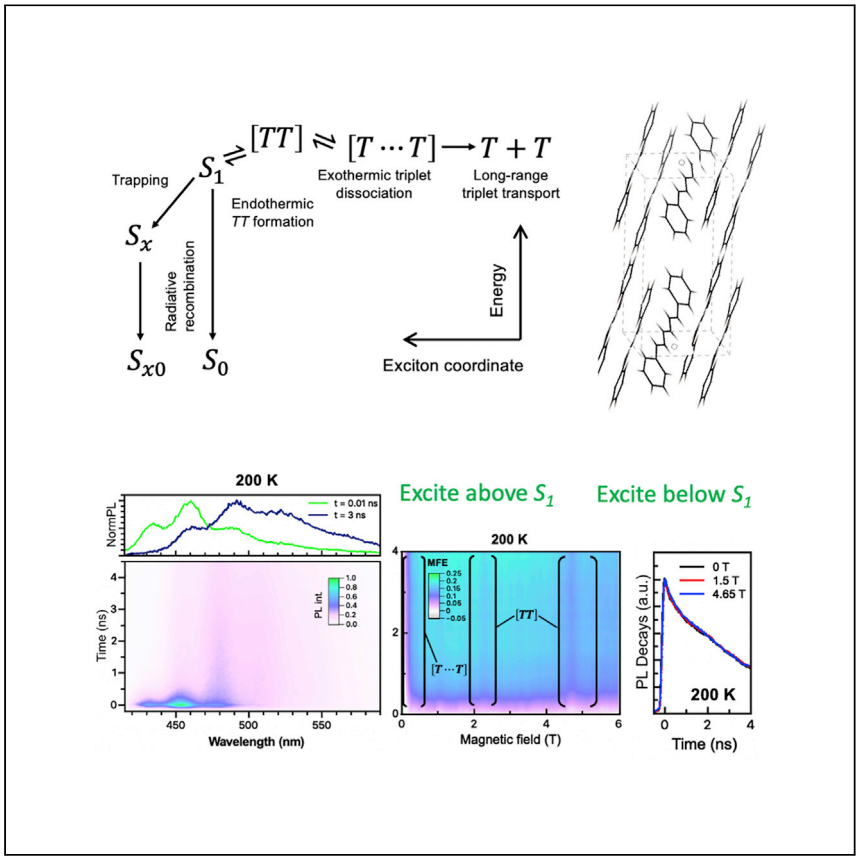

Using a refined magneto-optical transient experiment, Huang et al. show that the excimer-like delayed fluorescence can act as a competitive loss channel for triplet pair generation. The suggested experimental protocol in this work may help resolve the debate about the roles of intermediate states in singlet fission.

Yuqing Huang, Irina A. Buyanova, Chanakarn Phansa, ..., Akshay Rao, Weimin M. Chen, Yuttapoom Puttisong

yuttapoom.puttisong@liu.se

HIGHLIGHTS

Refined magneto-optical experiment reveals a loss channel for triplet pair generation

Excimer-like delayed photoluminescence in DPH crystal is a competitive loss channel

Generation of the triplet pair is endothermic, while its dissociation is exothermic

The bright trap state should be avoided in optimizing the singlet fission yield

Huang et al., Cell Reports Physical Science 2, 100339
February 24, 2021
https://doi.org/10.1016/j.xcrp.2021.100339

Cell Reports
Physical Science

CellPress
OPEN ACCESS

Article

Competition between triplet pair formation and excimer-like recombination controls singlet fission yield

Yuqing Huang,[1] Irina A. Buyanova,[1] Chanakarn Phansa,[2] Maria E. Sandoval-Salinas,[3,4] David Casanova,[3] William K. Myers,[5] Neil C. Greenham,[2] Akshay Rao,[2] Weimin M. Chen,[1] and Yuttapoom Puttisong[1,6,*]

SUMMARY

The ultimate goal for singlet fission is that each photo-excited singlet exciton, S_1, will result in two triplet excitons with unity yield. However, the singlet fission is now recognized to be complicated, involving bright/dark excited states of different spin multiplicity. Identifying the role of such states is vital to optimize singlet fission yield but difficult due to their elusive spectral signature. Here, we develop an experimental protocol based on a refined magneto-optical probe to access the fast time evolution of various excited states. In diphenylhexatriene crystal, the S_1 is found to undergo two competing processes—to form one of the two dark triplet pair intermediates having different exchange energies or to form a bright state, S_x, exhibiting excimer-like delayed photoluminescence. Our result provides a clear picture of a competition event in singlet fission, which is beneficial for the development and tailoring of singlet fission materials with high yield.

INTRODUCTION

Singlet fission, the process whereby a pair of triplet excitons is generated from a single singlet exciton formed by the absorption of one photon, has great potential for future optoelectronics that rely on exciton multiplication.[1–3] Over the past decade, our understanding of fundamental physics underlying the singlet fission has been advanced with the aid of careful analyses regarding spin physics,[4–13] electronic coupling, and electronic configuration.[13–24] However, the singlet fission yield in converting a photoexcited singlet exciton into two separated triplet excitons, [T + T], is still far from perfect. The difficulty of this task can be attributed to the complex nature of the singlet fission process. It involves many bright or dark excited states of different spin multiplicity along the singlet fission pathway that can be either essential or detrimental for generating free triplet excitons.[5,8,10,13–17,22,23,25–32] Special attention has been paid to the triplet pair states of multi-chromophore nature that are often called TT states.[15,22,28,30,32,33] Transient absorption/coherent vibrational studies suggest the TT states as the intermediates necessary for generating free triplet excitons.[28,32] The direct optical transition from TT to the ground state may also be probed as they gain a non-vanishing oscillator strength through a Herzberg-Teller-type mechanism[15] or breaking of symmetry in the case of intramolecular singlet fission in conjugated polymers.[34] These lead to excimer-like delayed photoluminescence (delayed PL). The excimer delayed PL has often been found in several tetracene derivatives[15,32,33] and in 3,6-bis(thiophen-2-yl)diketopyrrole derivatives.[35]

[1]Department of Physics, Chemistry, and Biology (IFM), Linköping University, Linköping, Sweden

[2]Cavendish Laboratory, University of Cambridge, J.J. Thomson Avenue, Cambridge CB3 0HE, UK

[3]Donostia International Physics Center (DIPC), Donostia, Euskadi, Spain

[4]Departament de Ciència de Materials i Química Física, Universitat de Barcelona, Barcelona, Catalunya, Spain

[5]Inorganic Chemistry, University of Oxford, Oxford, UK

[6]Lead contact

*Correspondence: yuttapoom.puttisong@liu.se

https://doi.org/10.1016/j.xcrp.2021.100339

However, the assignment of the excimer as a *TT* state and as a singlet fission precursor has been questioned by Dover et al.,[16] who argued based on kinetic analysis that the excimer in 5,12-bis((triisopropylsilyl)ethynyl)tetracene (TIPS-tetracene) behaves as a trap state.[16] We note that these discrepancies may stem partly from the state of the matter being probed (e.g., solid-state films[32] versus solution),[16] in which the excited states important for singlet fission may not necessarily be the same. Looking more broadly, delayed PL akin to the excimer emission in TIPS-tetracene is also found in tetracene crystals at low temperature, which was assigned to emission from defect states.[25,27] This complexity underlines the need to clarify the exact role of different excited states in the singlet fission pathway and for a better experimental protocol to differentiate them. Such knowledge is vital for the design and tailoring of materials to allow high singlet fission yield. It will then facilitate strategic design for both materials and optoelectronic device architectures.

To this end, spin-sensitive probes such as magneto-optical experiments and electron spin resonance (ESR) have been proven to be useful techniques in identifying *TT* intermediates through their characteristic spin-spin interactions.[4–8,10,11,36–43] In transient ESR (Tr-ESR) studies, the distinctive spin-resonance pattern was used to identify a set of *TT* intermediates with different exchange coupling strengths.[8,10,12,36] The coexistence of two triplet intermediates is also evident from magneto-optical studies of 1,6-diphenyl-1,3,5 hexatriene (DPH) crystals, as revealed by the magnetic field effect (MFE) on the steady-state PL.[6] Time evolution of Tr-ESR spectra provided a hint for the kinetic evolution between strongly interacting *TT* states and those that are spatially separated and non-interacting,[8,10,42] and on time-varying exchange coupling between pair of triplet excitons.[44] However, a complication in assigning the spin kinetics associated with *TT* intermediates to the delayed PL kinetics arises due to the different detection time windows of the two techniques. In typical Tr-ESR, the initial evolution of states within $t < 2–50$ ns is obscured by the instrumental response. This is problematic since the dynamic evolution of *TT* states, excimers, and other trap states is expected to occur on this timescale, taking crystalline film, disordered films, and solution of TIPS-tetracene at low temperatures as examples.[16,32,33]

Here, we present a refined magneto-optical mapping of Tr-PL, allowing us to probe the temporal evolution associated with two singlet excitons and two *TT* intermediates with a time resolution better than 2 ps. In combination with temporally and spectrally resolved PL measurements under selective optical excitation, the Tr-MFE allows us to differentiate between the dark intermediate *TT* and the bright singlet trap states responsible for the redshifted delayed PL. Our results demonstrate that the initially excited S_1 in the short polyene crystal shown in Figure 1A undergoes two competing processes, as represented in Figure 1B: (1) to form two *TT* intermediates with different exchange energies and (2) to form the bright trap state S_x that cannot regenerate *TT* pairs and, therefore, is detrimental to the overall singlet fission yield. Temperature-dependent Tr-MFE suggests endothermic singlet fission. Based on detail rate analysis, the endothermic step is between S_1 and the strongly exchange-coupled *TT* pairs [*TT*], whereas the dissociation from [*TT*] into a weakly exchange-coupled state [*T* … *T*] is exothermic. These two *TT* intermediates, together with S_1 and S_x, are dynamically linked due to cyclic singlet-exciton fission and triplet exciton refusion, which occur within 4 ns. The two triplet states, [*T* … *T*] and [*T* + *T*], differ as the former can undergo geminate refusion with a faster timescale and the latter is a long-range spatially separated state. Our results thus provide a more complete picture of the competing roles of the dark intermediate multi-exciton states

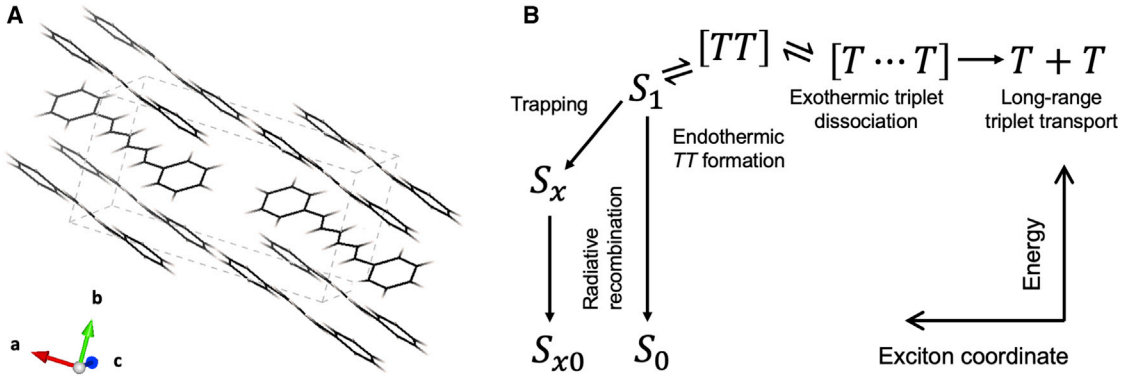

Figure 1. Singlet fission pathway in DPH monoclinic crystal

(A) Unit cell of DPH monoclinic crystal.

(B) Singlet fission pathway with 2 competing routes between formation of *TT* intermediates and the bright recombination hotspot S_x in a DPH monoclinic crystal. The energy ordering of the states reflects endothermic singlet fission and the trapping from S_1 to S_x.

and the trap states in determining singlet fission yield and offer a measurement protocol to differentiate them.

DPH polyene monoclinic crystals, as shown in the Figure 1A, were chosen as a typical example due to an advantage in the magneto-optical experiment. Their MFE patterns associated with both [*TT*] and [*T* … *T*] are expected within the range of applied magnetic fields B < 6 T.[6,36,45] These field conditions are accessible via a commercially available superconducting magnet. The MFE patterns of [*TT*] and [*T* … *T*] could be predicted using a classic Merrifield dynamic model with known spin Hamiltonian parameters, and the result is shown in Figure S1 for triplet conformation of both parallel and herringbone type. It shows the characteristic drops in PL yield, resulting from the singlet-quintet (S-Q) anti-crossing within the [*TT*] spin manifolds at B = 2.2 and 4.65 T. For the [*T* … *T*], the simulation predicts a well-known low-field MFE pattern in the range of B < 2 T. These two characteristic MFE patterns serve as fingerprints to identify the [*TT*] and [*T* … *T*] states in various magneto-optical experiments.[6,7,9,11,43,45,46]

RESULTS AND DISCUSSION

Delayed PL in DPH monoclinic crystal

Spectrally resolved Tr-PL at different temperatures was used to probe the dynamic evolution and population decay of the bright exciton states. Figures 2A and 2B show two-dimensional spectral/temporal PL profiles of the DPH crystal under 375-nm photoexcitation ($S_0 \rightarrow S_1$) at 200 and 8 K, respectively. Two exciton species can be identified by the observation of different exciton lifetimes at the long- and short-wavelength ranges of the probed spectral window. This is evident from the different PL spectra at t = 0.01 and 3-ns time delay shown in the upper panel of Figures 2A and 2B. Using a matrix reconstruction method with a genetic algorithm, one can separate the two excitonic species. The decomposition yields two components: the prompt PL from the S_1 state and the excimer-like delayed PL, assigned as the S_x state, as shown in Figures 2C–2F for temperatures of 200 and 8 K, respectively. By comparing the PL transition energy, the S_x state is estimated to lie 170 meV below the S_1 state. Apart from a slight modification of the 0-0 peak intensity, the overall PL features of S_1 and S_x at 200 and 8 K are quite similar. At 200 K, the S_1 state decays within a timescale of ~770 ps, together with a concomitant increasing population of the S_x state with a lifetime of ~4.6 ns. The population transfer between S_1 and S_x

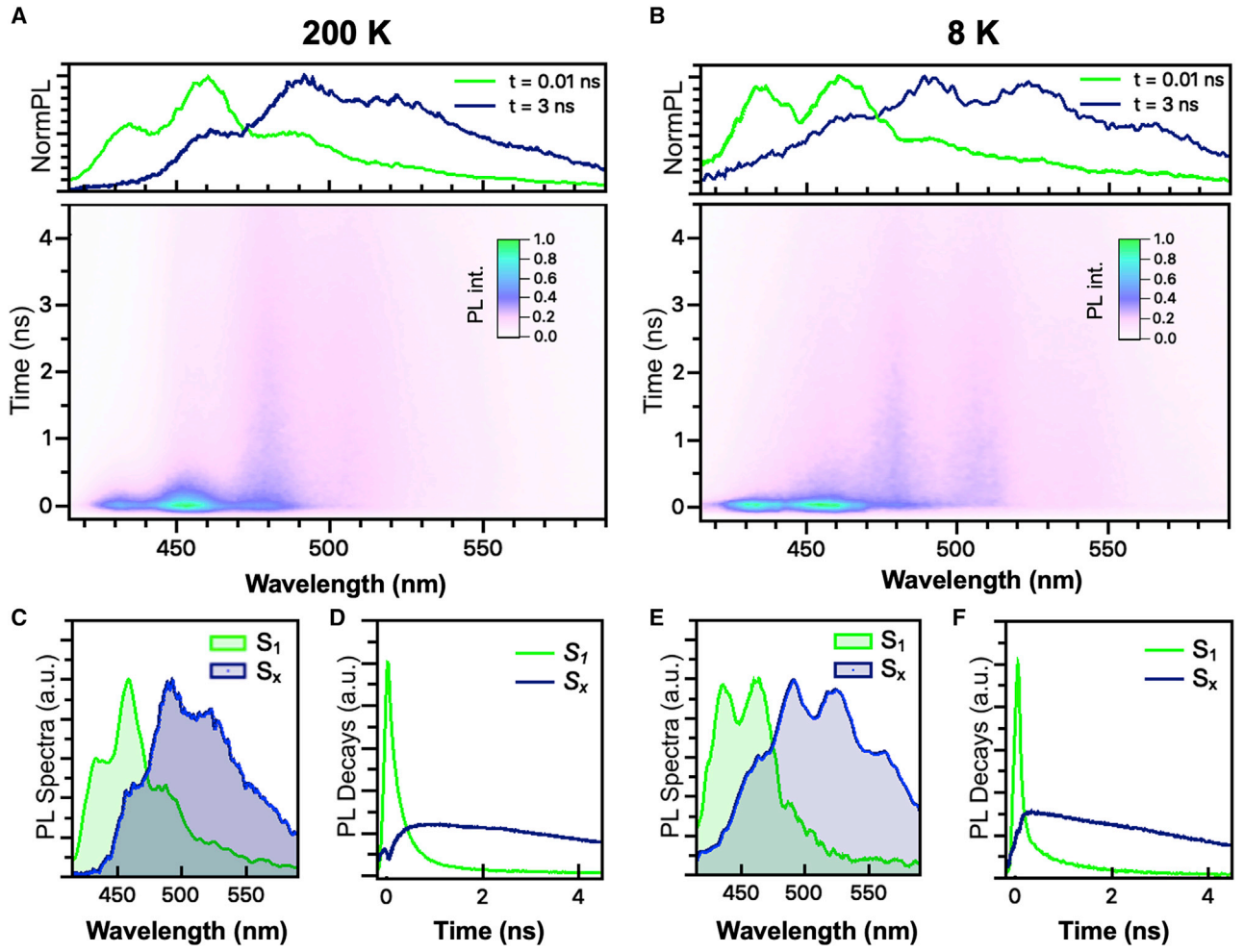

Figure 2. Temperature-dependent Tr-PL of the DPH crystal

(A and B) Spectrally resolved Tr-PL of the DPH monoclinic crystal at 200 and 8 K under 375 nm excitation ($S_0 \rightarrow S_1$ optical pumping), respectively. The normalized PL spectra at delay time t = 0.01 and 3 ns are plotted in the upper panel to illustrate the spectral evolution with time.

(C–F) Spectral and temporal decomposition of the spectrally resolved Tr-PL at 200 K (8 K) based on matrix reconstruction with intelligent genetic algorithm sampling.

states becomes faster at 8 K, with a timescale of ~80 ps. We attribute this to a coherence effect appearing at the temperature below 80 K (see further discussion in the Note S1 and Figure S2).

The delayed PL from S_x is of interest, as it resembles excimer delayed PL in TIPS-tetracene solid films and solution,[16,32,33] where there is controversy over whether it acts as a *TT* intermediate or a trap state. To examine the origin of S_x in DPH, we proceeded with fast magneto-Tr-PL experiments. This technique is capable of modulating excited species occupying different spin states through singlet fission/triplet refusion events, and detecting their evolution within the lifetime of the delayed PL.

Magneto-Tr-PL and MFE mapping: dynamic evolution of [*TT*] and [*T* … *T*] states

A schematic diagram of magneto-Tr-PL experiments is shown in Figure 3A. Here, the laser excitation and Tr-PL detection are parallel to the B field. The crystal surface normal is rotated 45° away from the optical axis to minimize laser scattering into

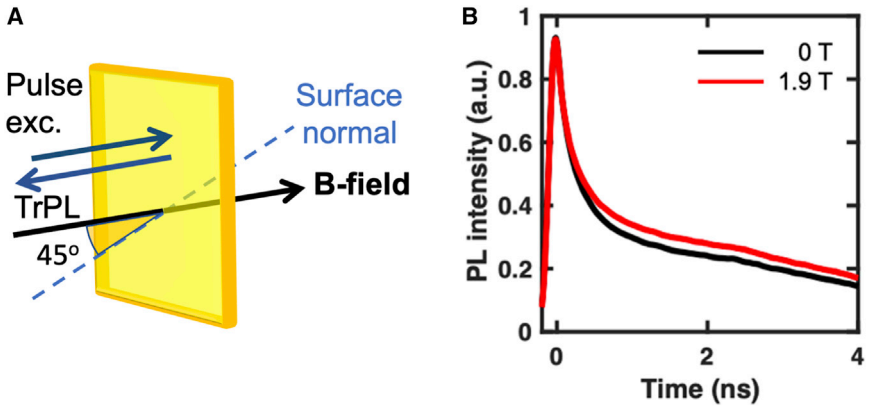

Figure 3. Magneto-Tr-PL of DPH crystal

(A) Experimental configuration of the magneto-Tr-PL experiments.

(B) Spectrally integrated Tr-PL measured at 200 K under 375 nm excitation and the detection spectral window of 415–600 nm. Magnetic field of B = 0 T (black) and B = 1.9 T (red) is applied.

the Tr-PL detection. This orientation also facilitates our later measurements under a quasi-resonant excitation condition. Figure 3B shows spectrally integrated Tr-PL (415–600 nm) measured at 200 K with a pulsed optical pumping to the S_1 state (375-nm excitation), at B = 0 T and 1.9 T. The fast and slow components of the Tr-PL are from S_1 and S_x states, respectively. The magnetic field response of the Tr-PL seen in Figure 3B is known to be a result of dynamic singlet fission and/or triplet-triplet refusion involving TT pair states.[38] Subsequently, the PL intensity $I(B,t)$ as a function of B field and time is carefully mapped out and translated into the mapping of Tr-MFE in Figure 4A by

$$MFE(B,t) = \frac{I(B,t) - I(0,t)}{I(0,t)}. \qquad \text{(Equation 1)}$$

This Tr-MFE mapping serves as a probe for the dynamic evolution of $[TT]$ and $[T \ldots T]$ states via their characteristic MFE fingerprint.

The contour color plots of Tr-MFE at 200, 100, and 8 K are shown in Figure 4A. The MFE fingerprints for the $[TT]$ and $[T \ldots T]$ states, as predicted in Figure S1, can be clearly seen in the MFE spectra at long delay times (t = 4 ns) in Figure 4B for T = 100 K and 200 K. The temporal evolution of the MFE fingerprints is clearly visible in Figure 4A within the marked magnetic field ranges. To quantify the temporal evolution of the two MFE fingerprints independently without interference, we introduce $MFE_{[T\ldots T]}(t) = MFE(B^{max}_{[T..T]}, t) - MFE(0,t)$ and $MFE_{[TT]}(t) = (MFE(B^{max}_{[TT]}, t) + MFE(B^{min}_{[TT]}, t))/2 - MFE(B^{c}_{[TT]}, t)$. Here $B^{max}_{[T..T]}$ = 1.7 T is the upper bound of the magnetic field required to produce the low-field MFE primarily dominated by ($[T \ldots T]$). However, $B^{min}_{[TT]}$ = 3 T and $B^{max}_{[TT]}$ = 6 T are, respectively, the lower and upper bounds of the field range associated with the high-field MFE produced by the S-Q anticrossing, centered around $B^{c}_{[TT]}$ = 4.65 T. The time evolutions of $MFE_{[T \ldots T]}(t)$ and $MFE_{[TT]}(t)$ at various temperatures are presented in Figures 4C and 4D.

We now consider the dynamics of the associated exciton species from the Tr-MFE results. We note that the origin of the Tr-MFE differs from other spin-sensitive transient probes. While techniques such as Tr-ESR monitor TT states ($S > 0$), formed directly from the singlet fission and/or indirectly via triplet-triplet annihilation in a bimolecular manner, Tr-MFE monitors these states through luminescence precursors such as S_1 and/or S_x. Therefore, finite MFE requires a complete circle of singlet fission and triplet

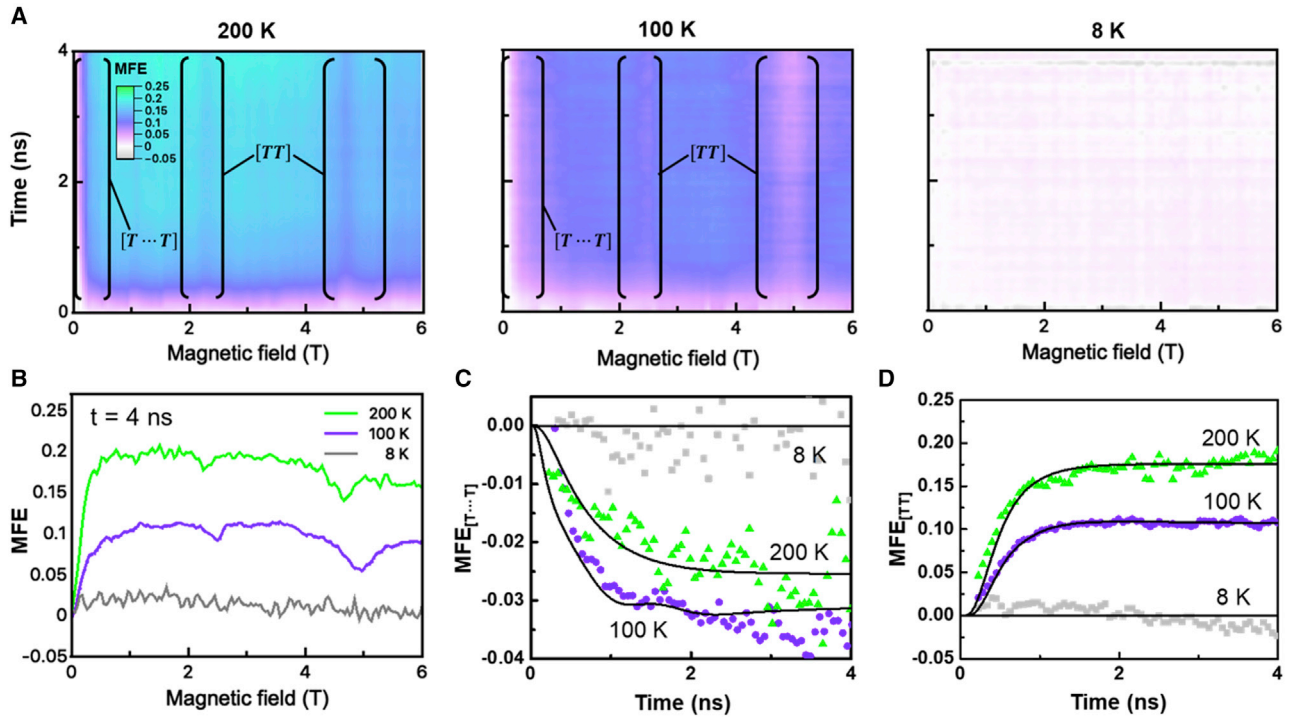

Figure 4. Temperature-dependent Tr-MFE spectra of DPH crystal

(A) Tr-MFE spectra measured from DPH monoclinic crystals under 375 nm excitation at 200, 100, and 8 K, respectively. The MFE patterns associated with [*TT*] and [*T* … *T*] are marked.

(B) The saturated MFE spectra taken at a delay time of t = 4 ns and temperatures of 200, 100, and 8 K.

(C and D) The time evolution of the $MFE_{[T \ldots T]}$ and $MFE_{[TT]}$, respectively, at different temperatures. The black solid curves are simulation results.

refusion. The Tr-MFE rises and saturates when a quasi-equilibrium between luminescence precursors and *TT* intermediates is established. The rise and the saturation of MFE features $MFE_{[T \ldots T]}$ and $MFE_{[TT]}$, as shown in Figures 4C and 4D, imply that a quasi-steady-state condition involving these two *TT* intermediates is established on similar timescales. In previous magneto-optical studies of DPH crystals at room temperature,[6,43,45] the MFE pattern was modeled by a stepwise process.[6,45] Namely, the singlet fission first generates [*TT*], which subsequently dissociates into [*T* … *T*] and [*T* + *T*] via triplet exciton migration. Within this framework, saturation of MFE indicates a quasi-equilibrium of $S_0 + S_1 \leftrightarrow [TT] \leftrightarrow [T \ldots T]$. Nonetheless, we can conclude that the generation and recombination of the two *TT* intermediates happen within 4 ns, which is similar to the time window in which the delayed PL from S_x is detected.

Next, we turn to the temperature dependence of the Tr-MFE. As can be seen from Figure 4, MFE becomes diminished as the temperature decreases from 200 to 8 K. Such observation may suggest an endothermicity of the singlet fission in the DPH monoclinic crystal.[38] Alternatively, it could indicate that the energy of the triplet pair states is below that of S_1. In this case, triplet refusion becomes improbable at low temperature, and, therefore, exothermic triplet pair states act as the non-radiative trap states. However, we argue that the exothermic case is not likely due to the following evidence. According to the temperature-dependent continuous wave (CW)-PL measurements shown in Figures S2A and S2B, an increase in optical transition yield from singlet states is observed at low temperatures. This rather supports the first endothermic scenario, in which the non-radiative competing singlet fission pathway is suppressed at low temperatures. At the same time, it goes against the

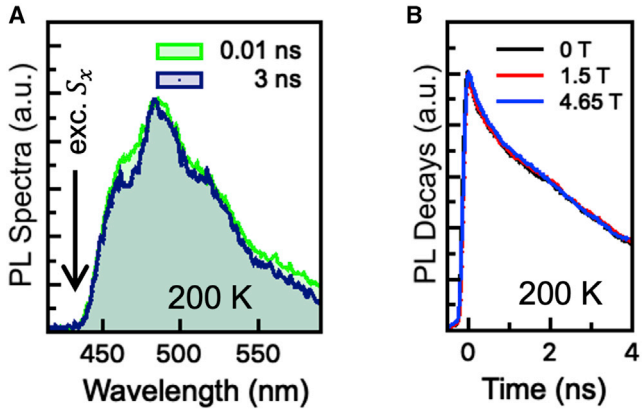

Figure 5. Vanished Tr-MFE under resonant excitation to S_x

(A) Tr-PL spectra taken at 0.01- and 3-ns time delays under the resonant excitation condition to S_x at 200 K.
(B) Tr-PL measured under resonant excitation to S_x at 200 K at different magnetic fields.

exothermic case, in which the formation of the triplet pair state acts as an efficient competing trap state, reducing optical transition yield. Later in the article, we show that a self-consistent rate-modeling analysis of temperature-dependent Tr-MFE provides further support for the endothermicity of the singlet fission process in DPH monoclinic organic crystals.

Dark TT intermediates and the bright recombination trap S_x

The fact that the two *TT* intermediates and the delayed PL (assigned to S_x) are present on similar timescales may imply that the S_x state is in fact a *TT* intermediate, provided that its optical transition is allowed via a Herzberg-Teller-type radiative transition.[15] However, the results from the Tr-MFE and the Tr-PL at 8 K do not support this assignment. At 8 K, the Tr-MFE shows that both [*TT*] and [*T* … *T*] could not be populated, while the S_x delayed PL is clearly seen (see Figure 2B). This discrepancy provides a hint that *TT* intermediates and the S_x are of different origins. To further justify this, magneto-Tr-PL under a selective optical excitation was used. Resonant excitation to S_x was achieved by tuning the excitation wavelength to be below the S_1 absorption edge. The fluorescence spectra at delay times of t = 0.01 ns and 3 ns under 430 nm excitation at 200 K are presented in Figure 5A. The fluorescence spectra in these two temporal windows, which correspond to the time windows in which the prompt and the delayed PL are respectively expected, exhibit no spectral evolution and are similar to the decomposed spectrum of S_x from Figure 2C. These confirm the resonant excitation to S_x. Importantly, the S_x decay curves under resonant excitation at 0, 1.5, and 4.65 T, shown in Figure 5B, do not exhibit any MFEs, despite the fact that strong MFEs associated with [*TT*] and [*T* … *T*] at 200 K were detected under non-resonant excitation (375 nm).

The disappearance of MFE under S_x resonant excitation implies that the states involving in the S_x radiative transition have a net zero magnetic moment. This experimental finding confirms that S_x is not a *TT* intermediate but a singlet state (S = 0) situated at ~170 meV below the S_1 state. We thus conclude that S_x acts as a competing recombination hotspot and the *TT* intermediates remain dark.

Self-consistent rate modeling and dynamic parameters evaluation of the trap state-induced singlet fission loss

To determine the important dynamic parameters and thus energy ordering along the singlet fission pathway, we perform detailed rate-modeling analysis of the

temperature-dependent Tr-MFE data based on the Lindblad master equation. This model follows the state-flow diagram shown in Figure 1. The detail analysis, values, and justification of fitting parameters can be found in Note S2 and Figure S3. In short, first, we restrict the fitting parameters to the minimum number of seven while using experimentally determined values for all of the remaining parameters. Second, we consider two conformations of the triplet pair states within the DPH monoclinic unit cells: the herringbone and the parallel configuration. Third, the fitting must have self-consistent fitting values of the Tr-MFE in all temperature ranges. Based on this fitting protocol, the analysis suggests that the singlet fission event most likely happens at the DPH pairs with a herringbone configuration, with a possible small contribution from that of the parallel configuration (see details in Note S2 and Figures S4 and S5). The fitting parameters are summarized in Table S1. In the case of herringbone structure, $S_1 \rightarrow [TT]$ has the endothermic barrier of $\sim\Delta_{SF}$ = 13.5 meV, and the endothermicity of the states is also in line with predictions from electronic structure calculations provided in Note S3 and Tables S4 and S5. We note that the theoretical absolute value of Δ_{SF} differs from the rate analysis due to intrinsic limitations of the computational model used (see Note S3 for a detailed discussion). The second step for triplet dissociation, $[TT] \rightarrow [T \ldots T]$, is found to be exothermic with $\Delta_{TT} = -12.4$ meV, in agreement with our highly correlated wave-function-based calculations (Table S3). The $[T \ldots T] \rightarrow [T + T]$ hopping dynamics γ_{TT}^{d} is set to be temperature independent, following a suggestion from a previous pioneer study in thin films of 6,13-bis(triisopropylsilylethynyl)pentacene, which was attributed to long-range triplet dissociation promoted by the vibronic effect.[40,47] The 8- to 200-K Tr-MFE fittings of the triplet pairs in the herringbone conformation are plotted as the black solid lines in Figures 4C and 4D.

The trapping from S_1 to S_x competes with the formation of TT intermediates, which lowers the overall singlet fission yield as S_x cannot regenerate TT pairs. To evaluate the competing loss, the dynamic parameters obtained from the rate modeling were used to estimate the singlet fission yield:

$$\Phi_{SF} = \frac{\gamma_{SF}}{(\gamma_{SF} + \gamma_{S1} + \gamma_{R})}, \qquad \text{(Equation 2)}$$

where γ_{SF}, γ_{S1}, and γ_R are the rate constants for singlet fission, $S_1 \rightarrow S_x$ trapping, and radiative recombination of S_1, respectively. This estimation considers an ideal condition with efficient separation and collection of fission-generated triplet excitons such that re-fusion is not likely.

Nonetheless, the obtained Φ_{SF} is still far from perfect. Φ_{SF} is found to be 0.79 (0.94), 0.69 (0.90), and 0 (<0.3) with (without) the contribution of the trap state, S_x, at 200, 100, and 8 K, respectively. This analysis shows that trapping to S_x happens on a timescale comparable to that of singlet fission and therefore must be avoided to promote a high singlet fission yield.

In general, the triplet refusion shall be also considered in determining the overall fission yield. Nevertheless, Φ_{SF} provides a good estimate of the efficiency of the singlet fission for devices with optimal performance. In the endothermic singlet fission process, it is natural to assume that the singlet fission rate γ_{SF} smaller than the reverse triplet fusion rate γ_{TF}. However, this does not necessarily imply a low fission efficiency. This is because the singlet fission efficiency is associated with the population flow (see Figure 1B) so that both the rate parameters (e.g., γ_{SF}, γ_{TF}) and occupation of the states (e.g., n_{S1} and $n_{[TT]}$ for S_1 and $[TT]$) matter. In optimized devices, the steady-state triplet or triplet pair density is assumed to be low due to the

efficient carrier extraction. The large concentration ratio between singlet and triplet pairs leads to a negligible exciton flow in the reverse direction. The fission efficiency is then only limited by the branching ratio between $S_1 \rightarrow [TT]$ that fission to triplet and $S_1 \rightarrow S_x$, which we denoted as trap state-induced singlet fission loss in this work. Therefore, Φ_{SF} reflects the fundamental singlet fission efficiency limited by the trap states S_x.

Regarding the possible origin of S_x, we consider both an excimer and crystal defects. The low emission energy and strong exciton-phonon coupling well resemble the excimer emission found in other organic crystals.[48] However, the intrinsic radiative lifetime of S_x (~4.7 ns) obtained from the Tr-PL analysis is rather short to be a dimeric/multi-chromophoric transition for an excimer. For the lattice defects, we consider the lattice imperfections due to misoriented minor conformers found from X-ray diffraction (XRD).[49] These defects, however, should be restored to normal lattice sites at low temperature.[49] Therefore, this type of lattice defect cannot account for the S_x delayed fluorescence, which appears at 8 K. Finally, we considered the PL of the *cis-trans* conformations of the molecule, which arise from rotation of the polyene carbon chain. The energy position and vibronic progression of the S_1 emission resemble the PL of the s-t-DPH conformer and those of the S_x emission resemble the PL of the s-c-DPH conformer.[50] Moreover, the ~170 meV redshift of S_x with respect to S_1 is in very good agreement with computed vertical energies (Table S2 and Table 1 in the previous first-principles study[51]). Thus, we tentatively attribute S_1 to the PL of s-t-DPH and S_x to the minority contribution of s-c-DPH.

In summary, the competing formation of dark *TT* intermediates and bright recombination hotspots, S_x, in singlet fission have been clearly demonstrated in DPH. S_x cannot regenerate *TT* intermediates and, therefore, is detrimental to the overall singlet fission yield. We conclude that the *TT* intermediates, both with strong and weak exchange coupling, are the necessary steps for free triplet generation. The temperature effects on the Tr-MFE reveal an endothermic singlet fission. Optimizing the singlet fission yield in endothermic systems should be done by avoiding the formation of low-energy bright states. We anticipate that our experimental protocols will help in resolving the debate about the roles of intermediate states and delayed PL in singlet fission materials more generally.

EXPERIMENTAL PROCEDURES

Resource availability

Lead contact

Further information and requests for resources should be directed to and will be fulfilled by the lead contact, Yuttapoom Puttisong (yuttapoom.puttisong@liu.se).

Materials availability

This study did not generate new unique reagents.

Data and code availability

The datasets generated, analyzed during the current study and the simulation code are available from the lead contact on reasonable request.

Sample preparation

DPH crystal powders were purchased from Sigma-Aldrich. The single monoclinic crystal was grown from a saturated DPH solution in dimethyl sulfoxide (DMSO). Monoclinic crystal structure was confirmed by X-ray diffraction experiment.

Spectral-resolved Tr-PL and transient magneto-optical experiments

Fast spectral-resolved Tr-PL was measured by a Hamamatsu Streak camera assembled with a single-grating monochromator. The optimal time resolution was better than 1 ps. The excitation source was a 76-MHz Ti:sapphire pulsed laser with a second harmonic generator to produce an excitation wavelength range of 360–430 nm. The pulse width was 150 fs. The excitation power was kept low throughout the measurement to minimize non-geminate triplet exciton re-fusion that could contribute to a long-lived delayed PL with t > 1 μs. The Tr-PL being probed in all of the experiments had an effective lifetime <13 ns, and therefore was of geminate type. The samples were placed inside a liquid-He superconducting magnet cryostat operated at T = 1.75–275 K and B = 0–10 T. The surface normal of the sample was oriented at 45° to the B field direction.

SUPPLEMENTAL INFORMATION

Supplemental information can be found online at https://doi.org/10.1016/j.xcrp.2021.100339.

ACKNOWLEDGMENTS

This work was supported by the starting grant of Y.P. from the Swedish Research Council (VR-2017-05285) and by Linköping University through the professor contracts of W.M.C. and I.A.B. Y.H. acknowledges financial support from the Knut and Alice Wallenberg Foundation (KAW). C.P. received funding from the Royal Thai Government Scholarship under the Development and Promotion of Science and Technology Talents Project (DPST). A.R. and N.C.G. acknowledge support from the EPSRC (EP/M005143/1 and EP/P027741/1). W.K.M. is supported by EPSRC grant no. EP/L011972/1 to the Centre for Advanced ESR. D.C. acknowledges financial support from Spanish Government MINECO/FEDER (project no. PID2019-109555GB-I00) and the Basque government (project no. PIBA19-0004). M.E.S.-S. acknowledges CONACYT-Mexico for a Ph.D. fellowship (ref. no. 591700).

AUTHOR CONTRIBUTIONS

Y.P. conceived the idea and designed the experiments. Y.P. prepared the samples. Y.H. and Y.P. performed the magneto-optical experiments and interpreted the data. C.P. performed the transient experiments. M.E.S.-S. and D.C. performed the electronic structure calculations. W.K.M. provided expertise in using/developing spin-sensitive probes. I.A.B., W.M.C., N.C.G., and A.R. oversaw the projects. Y.H. and Y.P. wrote the manuscript with input from all of the authors.

DECLARATION OF INTERESTS

The authors declare no competing interests.

Received: August 27, 2020
Revised: December 1, 2020
Accepted: January 15, 2021
Published: February 8, 2021

REFERENCES

1. Smith, M.B., and Michl, J. (2010). Singlet fission. Chem. Rev. *110*, 6891–6936.
2. Smith, M.B., and Michl, J. (2013). Recent advances in singlet fission. Annu. Rev. Phys. Chem. *64*, 361–386.
3. Rao, A., and Friend, R.H. (2017). Harnessing singlet exciton fission to break the Shockley–Queisser limit. Nat. Rev. Mater. *2*, 17063.
4. Merrifield, R.E. (1968). Theory of Magnetic Field Effects on the Mutual Annihilation of Triplet Excitons. J. Chem. Phys. *48*, 4318–4319.
5. Burdett, J.J., and Bardeen, C.J. (2012). Quantum beats in crystalline tetracene delayed fluorescence due to triplet pair coherences

produced by direct singlet fission. J. Am. Chem. Soc. *134*, 8597–8607.

6. Wakasa, M., Kaise, M., Yago, T., Katoh, R., Wakikawa, Y., and Ikoma, T. (2015). What Can Be Learned from Magnetic Field Effects on Singlet Fission: Role of Exchange Interaction in Excited Triplet Pairs. J. Phys. Chem. C *119*, 25840–25844.

7. Wang, R., Zhang, C., Zhang, B., Liu, Y., Wang, X., and Xiao, M. (2015). Magnetic dipolar interaction between correlated triplets created by singlet fission in tetracene crystals. Nat. Commun. *6*, 8602.

8. Weiss, L.R., Bayliss, S.L., Kraffert, F., Thorley, K.J., Anthony, J.E., Bittl, R., Friend, R.H., Rao, A., Greenham, N.C., and Behrends, J. (2016). Strongly exchange-coupled triplet pairs in an organic semiconductor. Nat. Phys. *13*, 176.

9. Bayliss, S.L., Weiss, L.R., Rao, A., Friend, R.H., Chepelianskii, A.D., and Greenham, N.C. (2016). Spin signatures of exchange-coupled triplet pairs formed by singlet fission. Phys. Rev. B *94*, 45204.

10. Tayebjee, M.J.Y., Sanders, S.N., Kumarasamy, E., Campos, L.M., Sfeir, M.Y., and McCamey, D.R. (2017). Quintet multiexciton dynamics in singlet fission. Nat. Phys. *13*, 182–188.

11. Bayliss, S.L., Weiss, L.R., Mitioglu, A., Galkowski, K., Yang, Z., Yunosova, K., Surrente, A., Thorley, K.J., Behrends, J., Bittl, R., et al. (2018). Site-selective measurement of coupled spin pairs in an organic semiconductor. Proc. Natl. Acad. Sci. USA *115*, 5077–5082.

12. Pun, A.B., Asadpoordarvish, A., Kumarasamy, E., Tayebjee, M.J.Y., Niesner, D., McCamey, D.R., Sanders, S.N., Campos, L.M., and Sfeir, M.Y. (2019). Ultra-fast intramolecular singlet fission to persistent multiexcitons by molecular design. Nat. Chem. *11*, 821–828.

13. Miyata, K., Conrad-Burton, F.S., Geyer, F.L., and Zhu, X.-Y. (2019). Triplet Pair States in Singlet Fission. Chem. Rev. *119*, 4261–4292.

14. Zimmerman, P.M., Zhang, Z., and Musgrave, C.B. (2010). Singlet fission in pentacene through multi-exciton quantum states. Nat. Chem. *2*, 648–652.

15. Yong, C.K., Musser, A.J., Bayliss, S.L., Lukman, S., Tamura, H., Bubnova, O., Hallani, R.K., Meneau, A., Resel, R., Maruyama, M., et al. (2017). The entangled triplet pair state in acene and heteroacene materials. Nat. Commun. *8*, 15953.

16. Dover, C.B., Gallaher, J.K., Frazer, L., Tapping, P.C., Petty, A.J., 2nd, Crossley, M.J., Anthony, J.E., Kee, T.W., and Schmidt, T.W. (2018). Endothermic singlet fission is hindered by excimer formation. Nat. Chem. *10*, 305–310.

17. Chan, W.-L., Ligges, M., Jailaubekov, A., Kaake, L., Miaja-Avila, L., Zhu, X.-Y., et al. (2011). Observing the Multiexciton State in Singlet Fission and Ensuing Ultrafast Multielectron Transfer. Science *334*, 1541–1545.

18. Chan, W.-L., Ligges, M., and Zhu, X.-Y. (2012). The energy barrier in singlet fission can be overcome through coherent coupling and entropic gain. Nat. Chem. *4*, 840–845.

19. Walker, B.J., Musser, A.J., Beljonne, D., and Friend, R.H. (2013). Singlet exciton fission in solution. Nat. Chem. *5*, 1019–1024.

20. Yost, S.R., Lee, J., Wilson, M.W., Wu, T., McMahon, D.P., Parkhurst, R.R., Thompson, N.J., Congreve, D.N., Rao, A., Johnson, K., et al. (2014). A transferable model for singlet-fission kinetics. Nat. Chem. *6*, 492–497.

21. Casanova, D. (2014). Electronic Structure Study of Singlet Fission in Tetracene Derivatives. J. Chem. Theory Comput. *10*, 324–334.

22. Bakulin, A.A., Morgan, S.E., Kehoe, T.B., Wilson, M.W., Chin, A.W., Zigmantas, D., Egorova, D., and Rao, A. (2016). Real-time observation of multiexcitonic states in ultrafast singlet fission using coherent 2D electronic spectroscopy. Nat. Chem. *8*, 16–23.

23. Monahan, N.R., Sun, D., Tamura, H., Williams, K.W., Xu, B., Zhong, Y., Kumar, B., Nuckolls, C., Harutyunyan, A.R., Chen, G., et al. (2017). Dynamics of the triplet-pair state reveals the likely coexistence of coherent and incoherent singlet fission in crystalline hexacene. Nat. Chem. *9*, 341–346.

24. Miyata, K., Kurashige, Y., Watanabe, K., Sugimoto, T., Takahashi, S., Tanaka, S., Takeya, J., Yanai, T., and Matsumoto, Y. (2017). Coherent singlet fission activated by symmetry breaking. Nat. Chem. *9*, 983–989.

25. Burdett, J.J., Müller, A.M., Gosztola, D., and Bardeen, C.J. (2010). Excited state dynamics in solid and monomeric tetracene: the roles of superradiance and exciton fission. J. Chem. Phys. *133*, 144506.

26. Zimmerman, P.M., Bell, F., Casanova, D., and Head-Gordon, M. (2011). Mechanism for singlet fission in pentacene and tetracene: from single exciton to two triplets. J. Am. Chem. Soc. *133*, 19944–19952.

27. Burdett, J.J., Gosztola, D., and Bardeen, C.J. (2011). The dependence of singlet exciton relaxation on excitation density and temperature in polycrystalline tetracene thin films: kinetic evidence for a dark intermediate state and implications for singlet fission. J. Chem. Phys. *135*, 214508.

28. Musser, A.J., Liebel, M., Schnedermann, C., Wende, T., Kehoe, T.B., Rao, A., and Kukura, P. (2015). Evidence for conical intersection dynamics mediating ultrafast singlet exciton fission. Nat. Phys. *11*, 352–357.

29. Monahan, N., and Zhu, X.-Y. (2015). Charge transfer-mediated singlet fission. Annu. Rev. Phys. Chem. *66*, 601–618.

30. Pensack, R.D., Ostroumov, E.E., Tilley, A.J., Mazza, S., Grieco, C., Thorley, K.J., Asbury, J.B., Seferos, D.S., Anthony, J.E., and Scholes, G.D. (2016). Observation of Two Triplet-Pair Intermediates in Singlet Exciton Fission. J. Phys. Chem. Lett. *7*, 2370–2375.

31. Morrison, A.F., and Herbert, J.M. (2017). Evidence for Singlet Fission Driven by Vibronic Coherence in Crystalline Tetracene. J. Phys. Chem. Lett. *8*, 1442–1448.

32. Stern, H.L., Cheminal, A., Yost, S.R., Broch, K., Bayliss, S.L., Chen, K., Tabachnyk, M., Thorley, K., Greenham, N., Hodgkiss, J.M., et al. (2017). Vibronically coherent ultrafast triplet-pair formation and subsequent thermally activated dissociation control efficient endothermic singlet fission. Nat. Chem. *9*, 1205–1212.

33. Stern, H.L., Musser, A.J., Gelinas, S., Parkinson, P., Herz, L.M., Bruzek, M.J., Anthony, J., Friend, R.H., and Walker, B.J. (2015). Identification of a triplet pair intermediate in singlet exciton fission in solution. Proc. Natl. Acad. Sci. USA *112*, 7656–7661.

34. Hu, J., Xu, K., Shen, L., Wu, Q., He, G., Wang, J.Y., Pei, J., Xia, J., and Sfeir, M.Y. (2018). New insights into the design of conjugated polymers for intramolecular singlet fission. Nat. Commun. *9*, 2999.

35. Mauck, C.M., Hartnett, P.E., Margulies, E.A., Ma, L., Miller, C.E., Schatz, G.C., Marks, T.J., and Wasielewski, M.R. (2016). Singlet Fission via an Excimer-Like Intermediate in 3,6-Bis(thiophen-2-yl)diketopyrrolopyrrole Derivatives. J. Am. Chem. Soc. *138*, 11749–11761.

36. Ishikawa, K., Yago, T., and Wakasa, M. (2018). Exploring the Structure of an Exchange-Coupled Triplet Pair Generated by Singlet Fission in Crystalline Diphenylhexatriene: Anisotropic Magnetic Field Effects on Fluorescence in High Fields. J. Phys. Chem. C *122*, 22264–22272.

37. Katoh, R., Hashimoto, M., Takahashi, A., Sonoda, Y., Yago, T., and Wakasa, M. (2017). Singlet Fission in Fluorinated Diphenylhexatrienes. J. Phys. Chem. C *121*, 25666–25671.

38. Dillon, R.J., Piland, G.B., and Bardeen, C.J. (2013). Different rates of singlet fission in monoclinic versus orthorhombic crystal forms of diphenylhexatriene. J. Am. Chem. Soc. *135*, 17278–17281.

39. Lubert-Perquel, D., Salvadori, E., Dyson, M., Stavrinou, P.N., Montis, R., Nagashima, H., Kobori, Y., Heutz, S., and Kay, C.W.M. (2018). Identifying triplet pathways in dilute pentacene films. Nat. Commun. *9*, 4222.

40. Matsuda, S., Oyama, S., and Kobori, Y. (2020). Electron spin polarization generated by transport of singlet and quintet multiexcitons to spin-correlated triplet pairs during singlet fissions. Chem. Sci. (Camb.) *11*, 2934–2942.

41. Sakai, H., Inaya, R., Nagashima, H., Nakamura, S., Kobori, Y., Tkachenko, N.V., and Hasobe, T. (2018). Multiexciton Dynamics Depending on Intramolecular Orientations in Pentacene Dimers: Recombination and Dissociation of Correlated Triplet Pairs. J. Phys. Chem. Lett. *9*, 3354–3360.

42. Nagashima, H., Kawaoka, S., Akimoto, S., Tachikawa, T., Matsui, Y., Ikeda, H., and Kobori, Y. (2018). Singlet-Fission-Born Quintet State: Sublevel Selections and Trapping by Multiexciton Thermodynamics. J. Phys. Chem. Lett. *9*, 5855–5861.

43. Wakasa, M., Yago, T., Sonoda, Y., and Katoh, R. (2018). Structure and dynamics of triplet-exciton pairs generated from singlet fission studied via magnetic field effects. Commun. Chem. *1*, 9.

44. Collins, M.I., McCamey, D.R., and Tayebjee, M.J.Y. (2019). Fluctuating exchange interactions enable quintet multiexciton formation in singlet fission. J. Chem. Phys. *151*, 164104.

45. Yago, T., Ishikawa, K., Katoh, R., and Wakasa, M. (2016). Magnetic Field Effects on Triplet Pair Generated by Singlet Fission in an Organic Crystal: Application of Radical Pair Model to Triplet Pair. J. Phys. Chem. C *120*, 27858–27870.

46. Merrifield, R.E. (1971). Magnetic effects on triplet exciton interactions. Pure Appl. Chem. *27*, 481.

47. Kobori, Y., Fuki, M., Nakamura, S., and Hasobe, T. (2020). Geometries and Terahertz Motions Driving Quintet Multiexcitons and Ultimate Triplet-Triplet Dissociations via the Intramolecular Singlet Fissions. J. Phys. Chem. B *124*, 9411–9419.

48. Seko, T., Ogura, K., Kawahami, Y., Sugino, H., Toyotama, H., and Tanaka, J. (1998). Excimer emission of anthracene, perylene, coronene and pyrene microcrystals dispersed in water. Chem. Phys. Lett. *291*, 438–444.

49. Harada, J., Harakawa, M., and Ogawa, K. (2008). Conformational change of all-trans-1,6-diphenyl-1,3,5-hexatriene in two crystalline forms. CrystEngComm *10*, 1777–1781.

50. Turek, A.M., Krishna, T.S.R., Brela, M., and Saltiel, J. (2016). Fluorescence excitation spectra of all-trans-1,6-diphenylhexatriene conformers: adiabatic conformer equilibration in the 21Ag state. Chem. Phys. Lett. *648*, 19–24.

51. Küpper, B., Kleinschmidt, M., Schaper, K., and Marian, C.M. (2011). On the photophysics of 1,6-diphenyl-1,3,5-hexatriene isomers and rotamers. ChemPhysChem *12*, 1872–1879.